Laser Ultrasonic Imaging Technique for Nondestructive Inspection of Defects in Three-dimensional Objects

_____

JUNJI TAKATSUBO*, SHIGEKI YASHIRO, BO WANG,

HIROSHI TSUDA AND NOBUYUKI TOYAMA

ABSTRACT:

We have developed a generation pulsed-laser scanning method for visualizing the propagation of ultrasonic waves. While scanning an object with a pulsed-laser beam to generate ultrasonic waves, we detected the propagated waves by means of a fixed PZT transducer. Although the detected waves were generated from different irradiation points, we were able to produce propagation images of the ultrasound generated at the reception-transducer position by applying simple data processing to the measured waveform data. This method has the following features that make it superior to the conventional visualization methods such as photo-elasticity method, Schlieren method, reception probe scanning method and computer simulation. (1) It enables us to visualize ultrasonic waves propagating on a complex-shaped object with curved surfaces, steps, and dents. (2) It makes high-speed imaging possible by use of mirror scan. (3) It provides excellent working efficiency by eliminating the need for adjustments to the laser incidence angle and the focal distance. (4) It has high detection sensitivity. (5) It enables us to remotely measure images of ultrasonic waves propagating over a wide area. By use of this laser ultrasonic system, we visualized the ultrasounds propagating around artificial defects, and examined the applicability of this method to nondestructive inspection of defects. The results demonstrate that this method is an effective means for quick detection of cracks, corrosions, debondings and delaminations in structures of steel and CFRP. The distinguishing features of this method are even applicable to field inspection work.

INTRODUCTION

In the field of ultrasonic flaw detection, the inspection of defects by observation and analysis of signal waveforms is common.   However, the propagation characteristics of

_____

*: National Institute of Advanced Industrial Science and Technology (AIST),RIIF,
Address: 1-1-1Umezono,Tsukuba,305-8568, Japan
E-mail: takatsubo.j@aist.go.jp

ultrasonic waves vary depending on the sensor type in use and its mounting state as well as on the sensor position and the material and dimension of the object inspected. In areas with complex shapes, reflected waves, diffracted waves, and mode-converted waves propagate while interfering with each other, making it difficult for even an expert inspector to accurately identify the echoes resulting from a defect within a short time. If it were possible to perform inspections while observing the propagation behavior of ultrasonic waves as images, the identification of echoes resulting from defects would become easier, and quicker inspection would become possible. Furthermore, fewer defects would be overlooked or improperly recognized, leading to higher-reliability inspections.

The Schlieren method [1-3] and the photo- elasticity method [4-5] are known methods for visualizing the propagation of ultrasonic waves. However, both of these are methods for visualizing ultrasonic waves propagating in transparent media and cannot be applied to opaque objects. Visualization by numerical analysis with computer simulation using the finite-element method has been implemented [6-9]. However, the necessary calculations are time consuming, even with the latest computers, so only objects with simple shapes can be analyzed. Furthermore, even if ultrasonic waves propagating on an object with a complex shape could be visualized using a high-performance computer, it is impossible to detect defects by simulation.

The detection laser scanning method [10,11] developed by us enables visualizing ultrasonic waves propagating on the surface of an opaque object. With this method, however, it is necessary to apply laser beams perpendicularly to the specimen and to keep the focal distance constant while scanning the object, making it difficult to visualize ultrasonic waves propagating on a 3-D object of arbitrary shape. We have recently developed a method [12] for visualizing the propagation of ultrasonic waves without detection laser probe but using generation laser. This method has the following features that make it superior to the conventional detection laser scanning method. (1) It enables us to visualize ultrasonic waves propagating on a complex-shaped object with curved surfaces, steps, and dents. (2) It provides excellent working efficiency by eliminating the need for adjustments to the laser incidence angle and the focal distance. (3) It makes high-speed imaging possible by use of mirror scan. (4) It has high detection sensitivity. (5) It enables us to remotely measure images of ultrasonic waves propagating over a wide area. For these reasons, we believe that this new method can be effectively applied to the inspection of defects in the field. In this study, we visualized the ultrasonic propagations around artificial defects in various specimens and examined the applicability of this method to non destructive inspection of flaws.

PRINCIPLE OF VISUALIZATION

When ultrasonic waves are detected propagating between two points using two transmission-reception sensors having the same frequency characteristics, the same waveform would be detected if the transmission-reception sensors replaced each other. Similarly, the waves detected by the piezoelectric sensor at point B from radiating laser beams at point A would be almost the same as the waves detected at point A from radiating laser beams at point B. The principle of the visualization of ultrasonic propagation is based on the proposition that the propagation of ultrasonic waves is
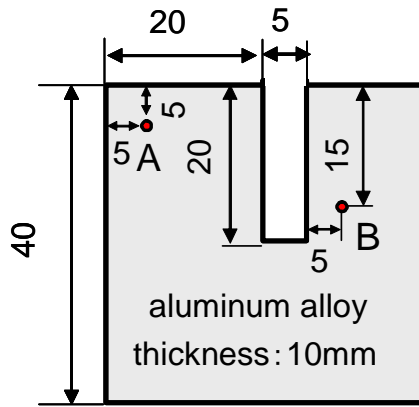
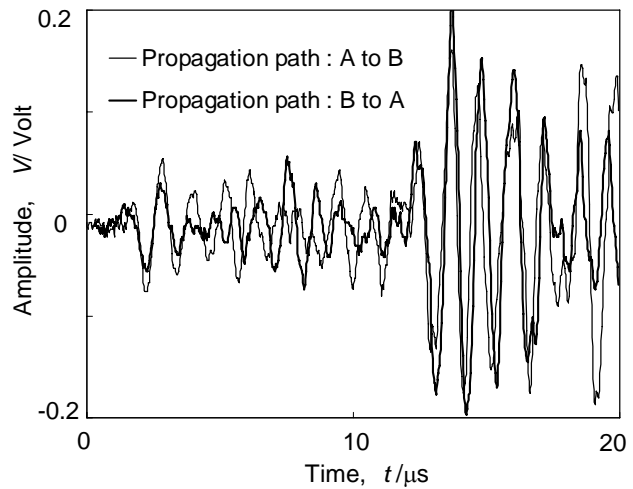Fig.1: aluminum alloy specimen with a notch

Fig.2: Comparison of waveforms when the propagation path between the laser radiation point and the reception PZT transducer position is reversed.

reversible. To confirm this reversibility, even when there is a defect in the propagation path of the ultrasonic waves, a notch with a width of 5 mm and a depth of 15 mm was made in an aluminum alloy specimen with a thickness of 10mm, as illustrated in Fig. 1. We then checked whether the ultrasonic waves detected by the piezoelectric sensor with an outer diameter of 3 mm mounted at point B with laser beams radiated from point A is equal to the waves detected by the piezoelectric sensor at point A with laser beams radiated from point B. As can be seen from Fig. 2, the two waveforms are almost the same. The lack of complete agreement between the two waves arises because it is difficult to mount the piezoelectric sensors with good reproducibility. In addition, the reversibility of propagation is not easily determined because the spot diameter of the laser beam (approximately 2 mm) differs from the diameter of the receiving section of the piezoelectric sensor (3 mm). The observed waveform is a Lamb wave with a velocity of about 2800 m/s.

If it is assumed that the propagation of ultrasonic waves is reversible, the train of waveforms detected by the fixed-position piezoelectric sensor during scanning by an oscillation laser (i.e. the aggregate of the waveforms detected at each scanning point) will be the same as the train of waveforms obtained by detecting the waves generated by directing laser beams toward the position of the piezoelectric sensor while scanning the sensor. Therefore, images may be created by modulating the amplitude of the train of waveforms detected during scanning by an oscillation laser. If these images are then displayed consecutively in the order of the measurement times, the resulting animation should show the propagation pattern at the time when laser-excited ultrasonic waves are oscillated at the fixed receiving point.

VISUALIZATION SYSTEM

An outline of the visualization system is presented in Fig. 3. Pulsed-laser beams (YAG 1064nm, pulse width 10 ns, beam diameter 2 mm, energy 5 mJ) are irradiated onto
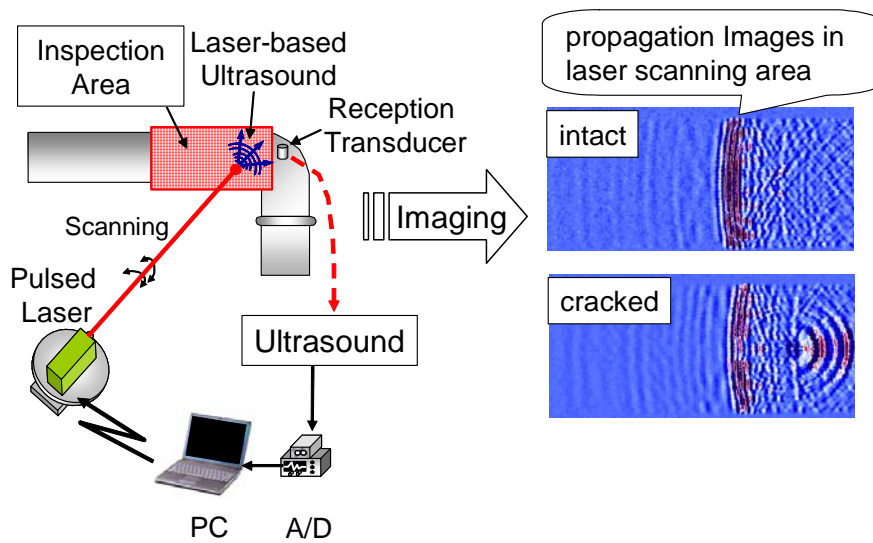
Fig. 3: Pulsed laser system for visualizing ultrasonic waves.

the specimen at a frequency of 20 Hz. The pulsed-laser oscillator is placed on a double-axle rotating stage and the irradiation point of the laser beams is scanned in the form of a grid by controlling the rotation angle of the stage with a PC. While scanning the measurement points arranged on a 100×100 grid for a total of 10,000 points, thermally excited ultrasonic waves generated at each irradiation point are detected by the receiving piezoelectric sensor and are recorded on the PC via an amplifier and digital oscilloscope (A/D converter). Because the amplitudes of these trains of waveforms at a given point in time correspond to the displacement of the ultrasound at each irradiation point if the reversibility of propagation of ultrasonic waves is utilized, images can be created whose intensities are determined by these amplitudes. When the images are displayed consecutively, the ultrasonic waves can be observed oscillating at the position of the receiving sensor. Although these images do not represent ultrasonic waves that are actually propagating, being based on actual measurement data, they are images of ultrasonic waves that can actually exist. The laser scanning and recording of the waveforms is performed at a rate of approximately 10 Hz, so it takes about 15 min to record the waveforms for 100×100 points.

EXAMPLES OF VISUALIZED PROPAGATION OF ULTRASONIC WAVES

Let us introduce a sample image of ultrasonic waves propagating on a drill as an example of the visualization of ultrasonic waves propagating on a 3-D object with a complex shape. As illustrated at the top (contour map of the ultrasonic amplitude) of Fig. 4, an ultrasonic transducer (diameter of the receiving section 4 mm, nominal resonance frequency 500 kHz) is mounted at the tip of the drill, and a 100 mm $\times$ 50 mm area was scanned by laser at intervals of approximately 0.5 mm (beam rotation pitch 0.025°) to obtain images of the propagation of ultrasonic waves. The laser beam is approximately 1 m long, the sampling interval of received waveform is 0.2μs, and the number of samples is 500. Figure 4 presents visualized images for each 5μs of propagation time. Although modeling ultrasonic waves propagating on an object of complex-spiral form seems to be

594

amplitude map

50

Transducer

angle beam transducer
（60°, 2.25MHz）

60

SUS304

t3.5

drilled holes（φ3, φ1）

5μs

longitudinal wave

surface wave

10μs

15μs

20μs

surface wave

longitudinal wave

5μs

10μs

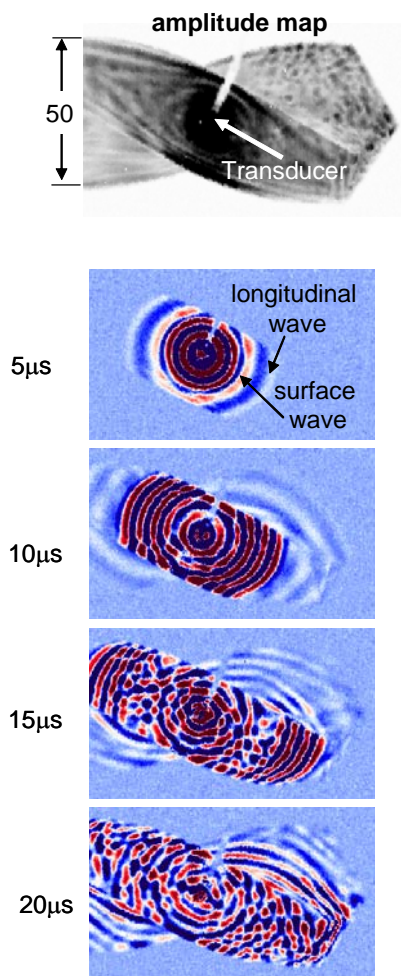dispersion from φ1 hole

15μs

dispersion from φ3 hole

20μs

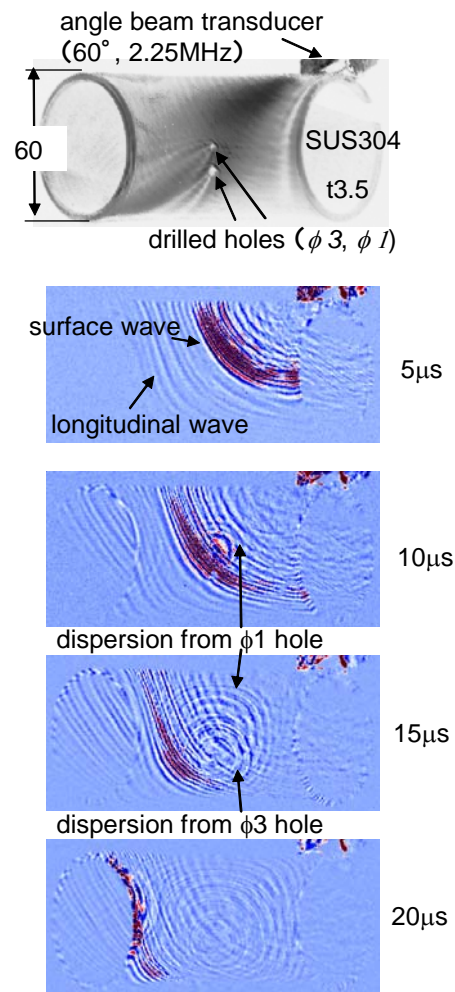Fig.4: Visualization of an ultrasonic wave propagating on a drill surface.

Fig. 5: Visualization of an ultrasonic wave propagating on a stainless steel elbow with drilled holes.

difficult even with computer simulation, visualization may be accomplished within a short time through the use of this technique.

We also investigated the visualization of ultrasonic waves propagating on a piece of stainless-steel elbow tube (50A) with two drilled holes having diameters of 1mm and 3mm. As illustrated at the top of Fig. 5, an angle beam transducer (60° incidence, nominal frequency of 2.25MHz) was mounted on the top end of the tube. A laser beam 1m in length scanned the surface of the tube at intervals of approximately 0.5mm (beam rotation pitch 0.025°) to generate ultrasonic waves, and the angle beam transducer detected the propagation waveforms. The received waveform sampling interval was 0.2μs, and the sampling number was 500 points. Figure 5 presents visualized images for each 5μs of propagation time. The ultrasonic waves passed through the 1mm hole and then dispersed (see the image for 10μs) and spread radially (see the image for 15μs). The second dispersion (see the image for 15μs) was observed when the ultrasonic wave passed through the 3mm hole. This result demonstrates the validity of the
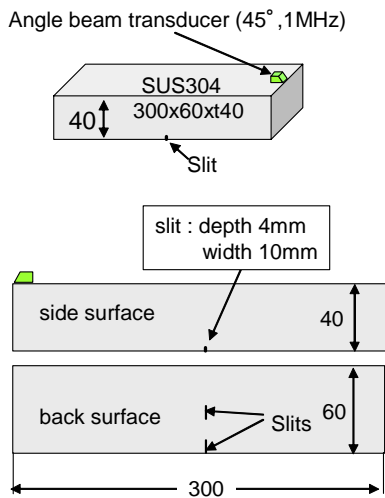
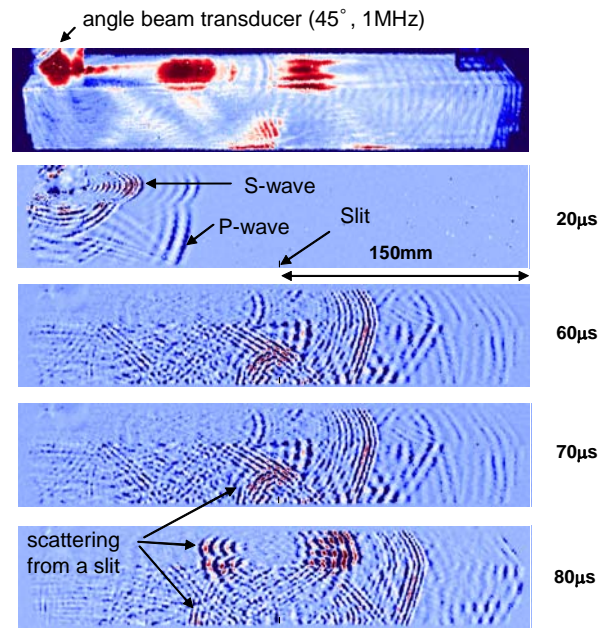Fig. 6: Thick plate of SUS304 steel with slits on the back surface.

Fig. 7: Visualization of the ultrasonic propagation in SUS304 steel with slits on the back surface.

ultrasonic visualization method for flaw inspections of 3-D objects with curved surfaces. Figure 5 (top) presents the contour map of the ultrasonic amplitude, in which shadow-like zones were observed at the backs of the drilled holes.

The next step was to visualize the scattering waves from slits on the back of a thick plate. Figure 6 depicts an SUS 304 stainless-steel plate 40mm thick with two slits on the back, 4mm deep and 10mm wide, provided for ultrasonic testing. An angle beam transducer (45° incidence, nominal frequency 1 MHz) was mounted on the end of the upper surface. Figure 7 presents the visualized result of the measurement of ultrasonic propagation on both top and side surfaces as well as the observed scattering from the slits on both surfaces. This result confirms the validity of ultrasonic visualization inspection as an effective means of explaining the ultrasonic propagation mechanism for detecting surface defects and it is applicable even to thick materials on the order of several tens of millimeters.

The final demonstration is ultrasonic propagation on a carbon fiber reinforced plastic (CFRP) structure. Figure 8 depicts a sample hat stringer of an airplane wing. Two PZT transducers were mounted on a hat and a stiffner as illustrated in Fig. 8. The area in the broken circle was debonded between the hat and the skin by chizeling. Although we inserted the chisel only a few centimeters inside the hat, the debonded area grew to about 5cm in length, as determined by ultrasonic C-scan imaging. Figure 9 shows the C-scan image of the waves propagating through the sample. Figure 10 presents the visualized propagation images at 20 μs intervals. The left figures show the propagation from PZT1, and the right figures show the propagation from PZT2. The debonded part forms a thin air layer, and ultrasonic waves have difficulty propagating across this layer. The debonded part and the intact part can thus be clearly distinguished. For ultrasonic testing, we used a band-pass frequency filter to produce a
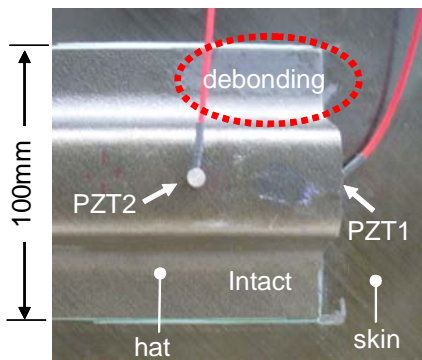
596

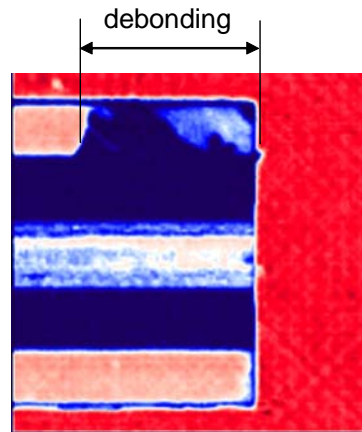Fig. 8: Sensor position on a sample CFRP hat stringer of an air plane wing.

Fig. 9: C-scan image of the sample CFRP hat stringer.

single-frequency ultrasound signal. The visualized signal in Fig. 10 is a single-frequency (300kHz) ultrasound signal, so there is very little velocity dispersion in the propagation image since such dispersion depends on frequency.

These results demonstrate that the ultrasonic visualization method is an effective means for nondestructive flaw inspection.

CONCLUSIONS

Our proposed method of ultrasonic visualization inspection uses thermally excited ultrasonic waves generated by scanning pulsed-laser beams over a specimen and visualizes the propagation of the resulting ultrasonic waves,
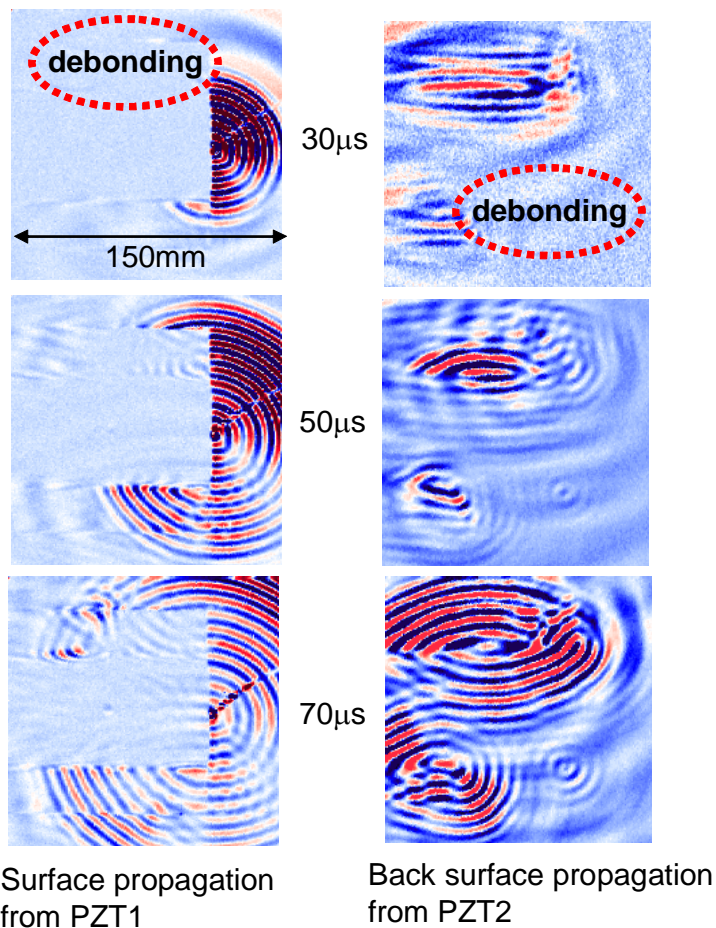

Surface propagation from PZT1

Back surface propagation from PZT2

Fig. 10: Ultrasonic propagation of the sample CFRP hat stringer.

597

based on the train of waveforms detected by a receiving sensor mounted at a fixed point. The conventional method, in which ultrasonic waves are visualized by scanning the detection laser probe, can only be used for objects that have flat surfaces, and it has very poor operability and work efficiency because of the need for sophisticated adjustment of the devices comprising the laser-optical system. This means that it can only be used to study ultrasonic waves in the laboratory. In contrast, the method proposed here enables the visualization of ultrasound propagating on a 3-D object with an arbitrary shape because of its capacity for efficient scanning. We used this visualization system to measure some images of ultrasonic propagation around artificial defects. The results demonstrate the validity of this method for nondestructive flaw inspection. In the near future, we will develop measurement systems that will enable higher-speed, higher-accuracy visualizations and will examine their possible uses in field inspections of piping and similar applications.

ACKNOWLEDGEMENTS

REFERENCES

1. K. L. Dilhan, Don-Liyanage and C. E. David: Appl. Phys. Lett. **79** 3356-3357. (2001)
2. M. A. Breazeale: J. Optics A, **3** ,1-7.(2001)
3. N. F. Declercq, A. Teklu, M. A. Breazeale, R. Briers, O. Leroy, J. Degrieck and G. N. Shkerdin: J. Appl. Phys., **96** ,5836-5840.(2004)
4. Y. H. Nam and S. S. Lee: J. Sound and Vibration, **259** ,1199-1207.(2003)
5. T. Mihara: Trans. of the Visualization Soc. of Jpn. (in Japanese), **118** ,181-186.(1988)
6. S. R. Ghorayeb, T. Xue, and W. Lord: *Review of Progress in Quantitative Nondestructive Evaluation*, **7B** , AIP, 1721-1728.(1988)
7. T. Hayashi and K. Kawashima: J. Acoust. Soc. Am., **113** , 1241-1248.(2003)
8. H. Yamawaki T. Saito: NDT & E Int., **33** ,489-497.(2000)
9. R. S. Schechter, K. E. Simmonds, N. K. Batra, R. B. Mignogna and P. P. Delsanto: Ultrasonics, **37** ,89-94.(1999)
10. J. Takatsubo M. Imade, Q. Fan and S. Yamamoto: Trans. of the Jpn. Soc. Of Mech. Engineers (in Japanese), **65**-C ,4299-4304.(1999)
11. J. Takatsubo and M. Imade: Trans. of the Visualization Soc. of Jpn. (in Japanese)，**22** ,23-27.(2002)
12. J. Takatsubo, B. Wang B, H. Tsuda and N. Toyama: Trans. of the Jpn. Soc. Of Mech. Engineers (in Japanese), **72**-718A ,945-950.(2006)